Dual-emission ratiometric fluorescence sensor based on CeO_2 quantum dots for the rapid detection of norfloxacin

M. M. Zhang [b], F. Peng [d], B. Z. Hu [e], Y. Lian [a,*], H. M. Wang [c], H. L. Wang [c]
[a] *College of Material and Textile Engineering, Jiaxing University, Jiaxing 314001, China*
[b] *Comprehensive Technology and Service Center of Jiaxing Customs, Jiaxing 314001, China*
[c] *College of Biological, Chemical Sciences and Engineering, Jiaxing University, Jiaxing 314001, China*
[d] *Comprehensive Technology and Service Center of Shaoxing Customs, Shaoxing 312000, China*
[e] *Technology Center of Hangzhou Customs, Hangzhou 310000, China*

The misuse and overuse of antibiotics brings serious pollution to the environment. Norfloxacin (NOR), one of the broad-spectrum antibiotics, is extensively used in treatment of human and animal diseases, which results in the continuous accumulation in the environment. Therefore, it is significance to develop a simple and efficient method for detecting norfloxacin. In this study, cerium dioxide quantum dots (CeO_2 QDs) with the characteristics of uniform size and excellent fluorescence emission property were synthesized by using the sol-gel method. A fast and ultrasensitive dual-emission ratiometric fluorescent sensor based on the CeO_2 QDs fluorescence was fabricated for the determination of norfloxacin, with a wide linear range (1.00-1000 nM), low detection limit of 0.65 nM, and fast response time (60 s). Furthermore, this ratiometric sensor has been applied for the determination of norfloxacin in environmental water samples with the recovery ranging from 95.54% to 101.04%, and the relative standard deviation 1.09% to 2.94%. these results are consistent with the results analyzed by the high-performance liquid chromatography (HPLC). Therefore, this as-presented sensor has a potential application in the determination of norfloxacin in environmental water samples.

(Received April 3, 2025; Accepted July 7, 2025)

Keywords: Ratiometric sensor, Norfloxacin, CeO_2 QDs, Rapid detection

1. Introduction

Antibiotics play a crucial role in modern medicine due to their efficacy in treating bacterial infections [1-4]. The primary antibacterial mechanism involves the inhibition of DNA gyrase, which disrupts bacterial DNA replication [5]. Recently, the misuse of antibiotics has garnered increasing public concern because of its significant threats to both human health and environmental integrity

* Corresponding authors: 85607385@qq.com
https://doi.org/10.15251/DJNB.2025.203.753

[6-8]. Norfloxacin (NOR), a synthetic broad-spectrum antimicrobial antibiotic, is widely employed in the treatment of enteritis, dysentery, and other diseases owing to its potent antibacterial properties and lack of cross-resistance with other antimicrobial agents [9]. Furthermore, NOR exhibits poor absorption and incomplete metabolism in humans and animals, leading to the persistent accumulation of its residues in the environment. These residues not only exert toxic effects on microorganisms, plants, and animals but also migrate into food sources and drinking water supplies, posing serious risks to public health [10]. Moreover, prolonged misuse of antibiotics can induce antibiotic resistance genes within bacterial populations as well as contribute to genetic pollution within ecological systems [11]. Consequently, there is an escalating focus on addressing environmental contamination resulting from antibiotic overuse. In light of this situation, it is particularly urgent to develop simple and rapid techniques that possess high sensitivity and selectivity for detecting trace levels of NOR in environmental water samples.

Hence, a variety of analytical approaches are employed to detect norfloxacin (NOR), such as chemiluminescence (CL) [12], immunoassays (IA) [13], high-performance liquid chromatography (HPLC) [14], surface-enhanced Raman spectroscopy (SERS) [15, 16], capillary electrophoresis (CE) [17], and fluorescence techniques (FL) [18-20]. Especially, fluorescence approaches attract increasing interest because of the simple manipulation, high sensitivity and fast response. However, most existing approaches rely on a single responsive signal for NOR detection, this can lead to signal fluctuations because of variations of the detection system as well as other external factors [21]. Fluorescence methods provide some merits including high accuracy, easy use and cost-effectiveness. They have found widespread application across various fields including environmental pollutant monitoring and biomedical assays. Among these methodologies, ratio-type fluorescent probes have attracted considerable interest because they can mitigate the influence of environmental variables through built-in calibration mechanisms. In contrast to single-emission fluorescence sensors that are susceptible to variations in probe concentration, excitation intensity, instrument efficiency, measurement conditions among other factors-, the ratio-type fluorescence sensor features two distinct emission peaks, which allows for comparative analysis based on the fluorescence signals from both peaks relative to the analyte concentration. Consequently, this approach effectively minimizes the impact of diverse external influences on test data while significantly enhancing detection accuracy.

A significant number of fluorescence methods with various fluorescent materials that display exceptional physicochemical characteristics, such as quantum dots (QDs) [22-24], metal-organic frameworks [25. 26], aggregation-induced emission (AIE) materials [27], which have been established for the detection of NOR. Among these diverse fluorescence materials, QDs have garnered considerable attention due to their tunable wavelength, excellent photochemical stability, favorable biocompatibility, and extended fluorescence lifetime. Consequently, they have been extensively employed to be sensor platforms. QDs can be fluorescent inorganic semiconductor nanocrystals with a diameter typically less than 10 nm. Due to quantum size as well as dielectric confinement effect, QDs possess specific optical and electrical properties. In comparison with other fluorescent materials, QDs offer numerous obvious merits like tunable fluorescence emission, great quantum yield, low toxicity, and resistance to photobleaching. Consequently, developing the more sensitive and accurate ratiometric fluorescence probes by leveraging novel fluorescent materials is imperative.

Recently, some inorganic fluorescent nanomaterials, such as QD, carbon dots, or metal (gold/silver) nanoclusters, garner growing attention. Because of their superb characteristics, like great photostability, potent fluorescence intensity, high size uniformity, ease of surface modification, along with wide wavelength tunability, QDs are regarded to be excellent fluorescent probes. To date, a variety of QDs have been synthesized and utilized in the detection of NOR; these include carbon dots (CDs) [28], sulfur quantum dots (SQDs) [22], graphene quantum dots (GQDs) [29], CdTe QDs [30], and CdTe/ZnS core/shell QDs [31]. However, each type of QD presents certain restrictions. CDs and GQDs exhibit low quantum yields (QY). Even though it is possible to enhance the QY through surface modification or heteroatom doping, such processes tend to be complex with low yield rates [32, 33]. For metal ion-based QDs like those based on cadmium compounds, challenges such as harsh preparation conditions, intricate reaction steps, high reagent costs, and significant toxicity hinder their widespread application [34]. Therefore, it is important to develop a cost-effective and green nano-optical materials to determine NOR.

As growing attention is paid to nanoparticles, metal oxides have emerged as particularly attractive materials for chemical sensors due to their favorable physicochemical properties and excellent biocompatibility. Inspired by previous studies, we synthesized novel cerium dioxide (CeO_2) quantum dots (QDs) by sol-gel approach for detecting norfloxacin (NOR). A ratiometric fluorescence sensing system on the basis of CeO_2 QDs was specifically proposed to detect NOR. The sensor exhibits two distinct emission peaks: one from the CeO_2 QDs and another from NOR itself. This innovative method was successfully applied to detect NOR in lake and river water samples, yielding good outcomes. As suggested by these findings, those synthesized CeO_2 QDs hold significant potential for determining NOR concentrations in environmental water samples. In light of the growing attention to nanoparticles, metal oxides have been particularly appealing for developing chemical sensors owing to their advantageous physicochemical characteristics and remarkable

In this study, we present a novel CeO_2 QDs for the detection of NOR utilizing a sol-gel approach, inspired by previous findings. To detect NOR, we developed a ratiometric fluorescence sensing device based on CeO_2 QDs. The emission peaks of the ratiometric fluorescence sensor are attributed to both the CeO_2 QDs and the NOR itself. This method was successfully employed to probe NOR in lake and river water samples, yielding good outcomes. Based on these findings, those developed CeO_2 QDs hold significant potential for determining NOR concentrations in ambient water samples.

2. Experimental

2.1. Materials and instrumentals

Tris(hydroxymethyl)aminomethane (Tris) was purchased from Sangon Bioengineering (Shanghai) Co. Ltd. Hydrochloric acid was obtained from Sinopharm Chemical Reagent Co. Ltd. Norfloxacin, sodium hydroxide, cerium nitrate hexahydrate ($Ce(NO_3)_3·6H_2O$), urea, polyvinyl alcohol(1750±50) (PVA), nitric acid (65.0~68.0%), norfloxacin (NOR), Moxifloxacin (MOX), prulifloxacin (PRFX), gatifloxacin (GTFX), sfloxacin(OFL), sparfloxacin (SPX), oxytetracycline (OTC), sulfadimethoxine (SDM), amoxicillin trihydrate (AMX), vancomycin hydrochloride (VAN), erythromycin (ERY), ~~3~~roxithromycin (ROX), chloramphenicol (CAP), sodium chloride, potassium

chloride, magnesium chloride, ferric chloride trihydrate, calcium chloride, ammonia (28.0~30.0%), anhydrous ethanol and hydrogen peroxide (30%) were provided by Shanghai Aladdin Bio-chemical Technology Co. Ltd. The lake, river, and tap water was sampled in Jiaxing City. The ultrapure water (18.2 mΩ·cm) utilized during experimental procedures was acquired from the Millipore water purification system of our laboratory. Every reagent was analytically pure and utilized as received.

We measured fluorescence spectra using the F-7000 spectrofluorometer (Hitachi, Japan). CeO_2 QDs morphology was examined with the JEM-2100F transmission electron microscope (JEOL, Japan). The XRD-7000 X-ray diffractometer (Shimadzu, Japan) was employed for obtaining X-ray diffraction (XRD) patterns. The Escalab 250Xi photoelectron spectrometer (Thermo Fisher Scientific, USA) was applied in conducting X-ray photoelectron spectroscopy (XPS). All liquid chromatography analyses were performed using a 1260 high-performance liquid chromatography system (Agilent, USA).

2.2. Synthesis of CeO_2 QDs

The polyvinyl alcohol (PVA) (10 m/v %) was obtained. Briefly, we introduced PVA (1750 ± 50) (2.0 g) and 20 mL deionized water in the 100 mL round-bottom flask. Then, the mixture was heated to 95 ℃ under vigorous stirring until the solution turned transparent. We synthesized CeO_2 QDs by sol-gel approach after some modifications based on the literature previously reported [35, 36]. Specifically, cerium nitrate hexahydrate (0.8484 g) and deionized water (20 mL) were brought into the 100 mL round-bottom flask with 5 min of slow stirring. Then, 1 mL hydrogen peroxide (30%) was added to this mixture drop by drop under vigorous stirring. Solution color altered from colorless at first to bright yellow and then light brown. Subsequently, 3.0 mL of ammonia (28.0~30.0%) was added rapidly to the mixture, resulting in the immediate formation of a substantial reddish-brown precipitate. This mixed solution was later subjected to heating at temperatures between 85 ℃ and 95 ℃, during which the solution gradually transitioned to a light yellow hue. This mixed solution underwent filtering thereafter, followed by dispersion of the precipitate within 20 mL deionized water; while the nitric acid aqueous solution (v/v=1/5) was used to adjust solution pH. This resultant mixes sample subsequently underwent heating till it attained a yellow-green coloration. Later, 2.0 mL PVA aqueous solution (10% w/v) was then added dropwise while stirring for an additional 5 min. Following this step, 2.0 mL urea aqueous solution (5% w/v) was introduced into the mixture while continuing stirring and refluxing for thirty minutes. Finally, after filtration and washing using deionized water, this precipitate underwent dispersion within 20 mL of anhydrous ethanol prior to storage under a temperature of 4 ℃.

2.3. Optimization of experimental conditions

The analysis conditions including the equilibrium time and pH were optimized. The CeO_2 QDs concentration diluted with 10 mM Tris-HCl buffer solution (pH 6.0) was set as 1.0 $\mu L \cdot mL^{-1}$. The fluorescence spectra of the mixture of 1.0 mL CeO_2 solution (1.0 $\mu L \cdot mL^{-1}$) and norfloxacin (10 nM) varied with the equilibrium time ranging from 0.25 min to 15 min were recorded. The influences of the pH values ranged from 3.0 to 6.0 on the fluorescence intensity ratio were evaluated.

2.4. Fluorescence detection for norfloxacin

The CeO_2 QDs solution at a concentration of 1.0 $\mu L \cdot mL^{-1}$ was obtained by dispersing the stock solution within the 10 mM Tris-HCl buffer solution (pH 6.0). Subsequently, 1.0 mL of the

CeO_2 QDs solution was transferred into a plastic centrifuge tube with a capacity of 1.5 mL. Different concentrations of norfloxacin solutions were then introduced into the tube, with total volume being adjusted to 1.5 mL. The fluorescence spectra were recorded following 1 min of equilibration under ambient temperature.

2.5. Selectivity analysis

The selectivity experiment was conducted by mixing various potential interferents including some the structural analogs and the inorganic salts. The measurements of the fluorescence spectra were consistent with the above-described procedures.

2.6. Detection of norfloxacin in water samples

The river, lake, and tap water was sampled in Jiaxing City and filtered using 0.22 μm filter membranes for eliminating suspended substances. Waste water obtained from the Zhejiang Environmental Monitoring Center underwent a similar filtration process. Prior to analysis, all water samples were diluted 100-fold with 10 mM Tris-HCl buffer solution (pH=6). Following these treatments, no norfloxacin was detected in the samples. Subsequently, we spiked tested water samples of varying concentrations of standard norfloxacin solutions (50, 200, and 600 nM). The recovery experiments adhered to the aforementioned procedures.

2.7. HPLC analysis conditions

The 1260 series HPLC system (Agilent, USA) was used for the analysis of NOR. The column was a C_{18} (5 μm, 4.6 mm × 15 cm). Acetonitrile (70%) and H_2O (30%) (H_3PO_4 adjusted pH=3.5) were the mobile phase at the 0.5mL min-1 controlled flow rate. The injection volume and temperature were 10 μL and 25 °C, respectively. Excitation (λ_{ex}) and emission (λ_{em}) wavelengths were 277 and 441nm), respectively.

3. Results and discussion

3.1. Design strategy of dual-emission ratio fluorescence sensor for norfloxacin detection

The ratio fluorescence sensor strategy in detecting NOR can be observed from Scheme1. When CeO_2 and Norfloxacin exist individually, there is only one emission peak excited at 263 nm, which is 350 nm and 440 nm respectively. And when CeO_2 and norfloxacin coexist, the emission peaks at 350 nm and 440 nm also exist. According to above-mentioned, we proposed a dual emission ultrasensitive ratio fluorescent sensor for the rapid detection of norfloxacin. The linearity of F_{440}/F_{350} with norfloxacin concentration was obtained by fixing the CeO_2 QDs concentration and gradually increasing norfloxacin concentration and the linear relationship can be used to detect norfloxacin. F_{440}/F_{350} means the ratio of emission peak fluorescence intensity between norfloxacin and CeO_2 QDs at the same excitation wavelength.

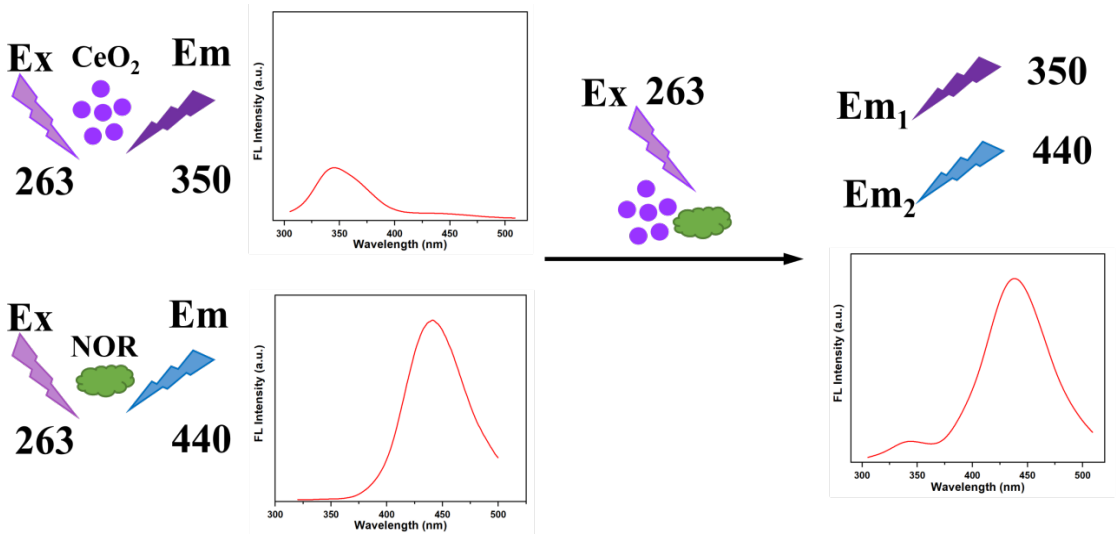

Scheme 1. Schematic illustration of the procedure for detecting norfloxacin.

3.2. Characterization of CeO_2 QDs

Transmission electron microscopy (TEM) images were utilized to characterize CeO_2 QDs morphology and size. As shown in Fig. 1A, the images of CeO_2 QDs uniform distribution were obtained, with diameters being 0.1~1.1 nm, while the greatest percentage being 0.4-0.6 nm in Fig. 1C. After over 100 particles were statistically analyzed, the mean CeO_2 QDs size was 0.52 nm. HR-TEM images for CeO_2 QDs (Fig. 1B) displayed the distinct lattice structures, with lattice parameter being 0.31 nm, probably associated with (111) diffraction planes of CeO_2 QDs. Fig.1D displays XRD patterns for CeO_2 QDs, with 5 diffraction peaks at 28.5°, 47.5°, 56.3°, 69.4° and 76.7° being associated with (111), (220), (311), (400), and (331) planes of CeO_2's cubic fluorite structure. Such planes can be excellently matched with examples in ICSD card 43-1002. Besides, the wide and weak reflection peaks are indicative of QD nanomaterials.

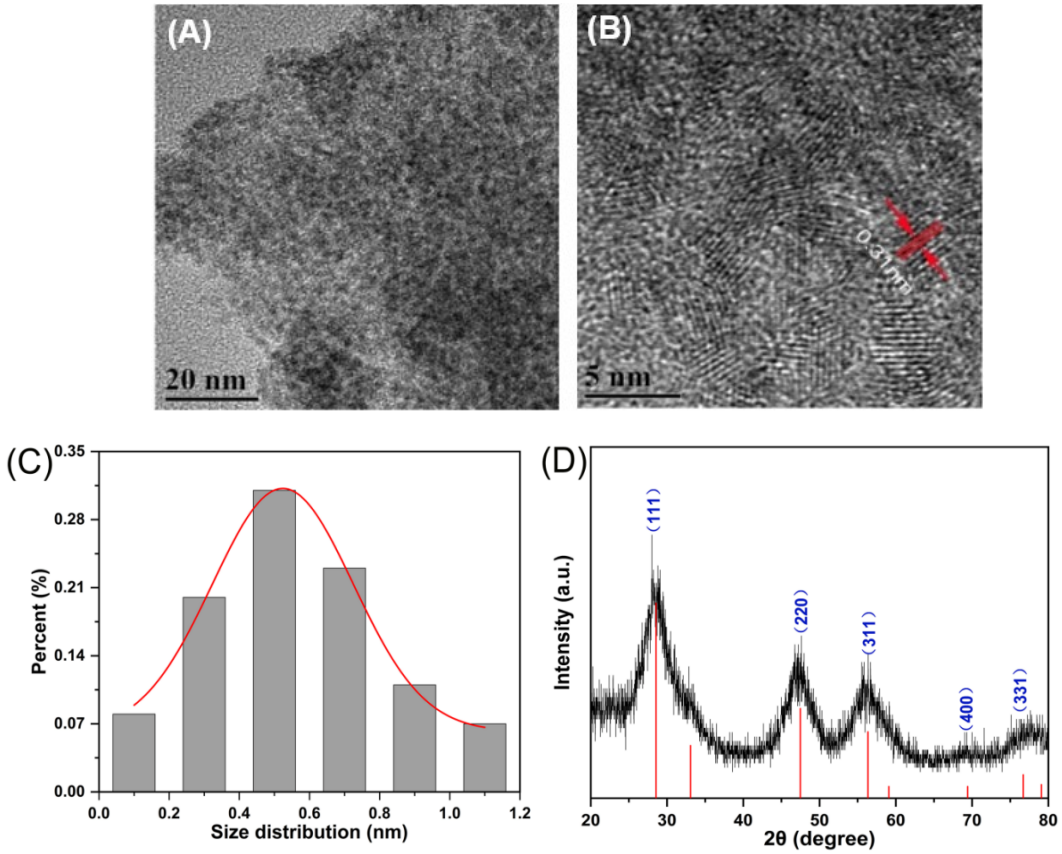

Fig. 1. Morphological characterization of CeO_2 QDs: (A) TEM image, (B) High resolution-TEM image, and (C) size distribution from TEM analysis, (D) XRD analysis of CeO_2 QDs.

XPS was conducted to analyze CeO_2 QDs for their electronic states and chemical compositions. XPS survey spectrum (Fig. 2A) shows the composition of elements Ce, O, and C. Moreover, Ce 3d XPS spectrum (Fig. 2B) reveals four major peaks of Ce^{4+} and Ce^{3+}. Peaks at 898.3 eV and 916.8 eV are associated with the $3d_{5/2}$ and $3d_{3/2}$ states for Ce^{4+}, while those at 882.4 eV and 900.9 eV can be attributed to the same states for Ce^{3+}. Two satellite peaks appear at 887.1 eV and 907.6 eV. From Fig. 2C, C 1s XPS spectrum was deconvolved into different carbon environments, with peaks measured at 284.7 eV and 286.2 eV being associated with C=C and C-C bonds in PVA stabilizers, respectively, while that at 288.5 eV was associated with C=O bond of unreacted urea. Besides, O 1s XPS spectrum (Fig. 2D) displays two peaks at 529.6 eV and 532.6 eV, associated with lattice oxygen related to CeO_2's crystal structure and hydroxyl oxygen related to PVA stabilizers, respectively. These findings align with previous research on CeO_2 nanoparticles.

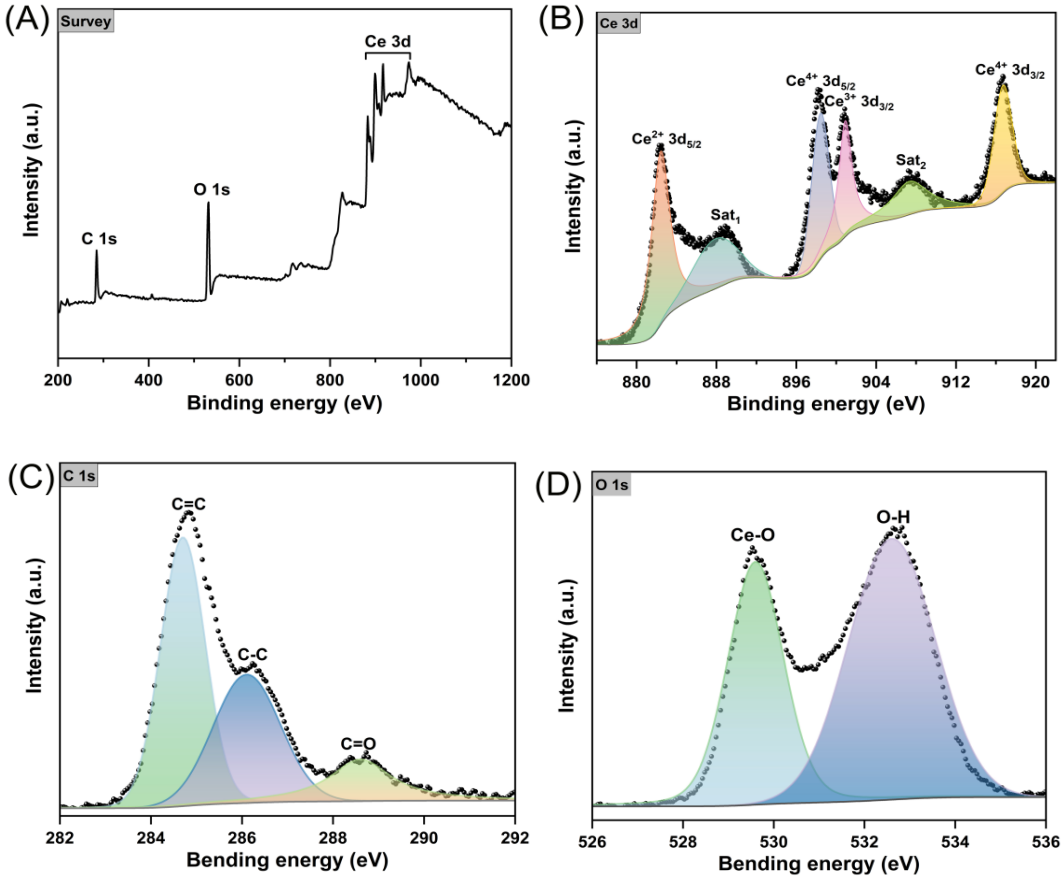

Fig. 2. XPS characterization of CeO_2 QDs: XPS survey spectra (A), the high-resolution Ce 3d (B), C 1 s (C), and O 1 s (D).

3.3. Optical property of CeO_2 QDs

From Fig. 3A, CeO_2 QDs show pronounced fluorescence associated with the distinctive quantum size effect. The fluorescence emission intensity initially elevates and subsequently declines at the excitation wavelength of 235-270 nm. Optimal excitation and emission wavelengths can be determined at 255 and 350 nm, separately. Nevertheless, at CeO_2 QDs' optimum excitation wavelength, fluorescence intensity of norfloxacin is not the strongest. Therefore, we obtained the excitation spectra of CeO_2 QDs and norfloxacin, as shown in Fig. 3B, there is a coincidence point at 263 nm, and CeO_2 QDs and norfloxacin have relatively strongest fluorescence intensity at this excitation wavelength. Therefore, 263 nm will be used as the excitation wavelength for subsequent experiments.

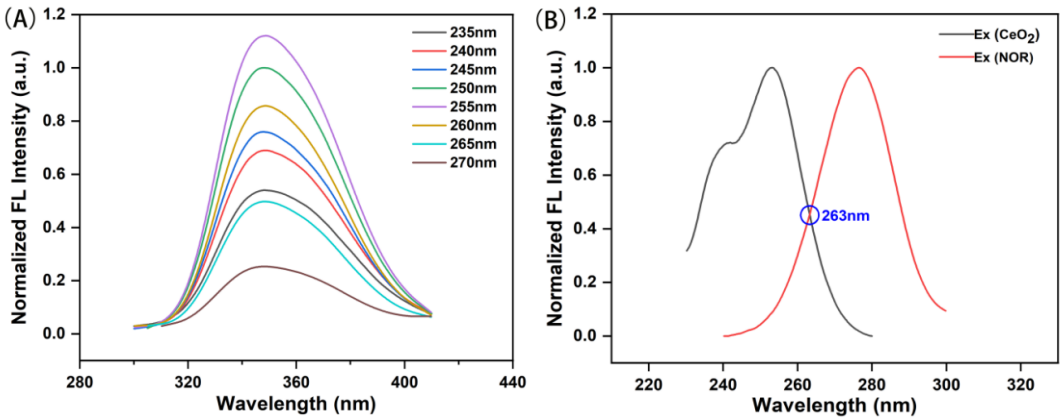

Fig. 3. (A) Emission spectra of CeO_2 QDs excited at different wavelengths in the range of 235~270 nm; (B) Photoluminescence excitation (PLE) spectra of CeO_2 QDs and norfloxacin.

3.4. Optimization of experimental conditions for norfloxacin detection

Two essential experimental conditions were comprehensively analyzed for obtaining best sensing property of ratiometric sensor in detecting norfloxacin. To start with, the concentration of CeO_2 QDs and norfloxacin were set to 1 $\mu L \cdot mL^{-1}$ and 10 nM, while additional experimental factors like equilibration time (A) and pH (B) were optimized. As shown in Fig. 4A, F_{440}/F_{350} values first were enhanced gradually and then decreased with the equilibrium time of CeO_2 QDs and norfloxacin, and F_{440}/F_{350} value was reached the maximum at 60 s. According to the previous report, CeO_2 QDs's fluorescence property is instable[36]. When pH is greater than 6, CeO_2 QDs have gradually decreased fluorescence intensity as pH elevates. For this reason, we only optimized the effect of pH=3~6 on F_{440}/F_{350}. The F_{440}/F_{350} value remains largely unchanged as pH elevates, as Fig. 4B shows. Therefore, the impact on the sensing performance of the pH to ratio sensor can be not take into account, and subsequent experiments were conducted at pH=6.

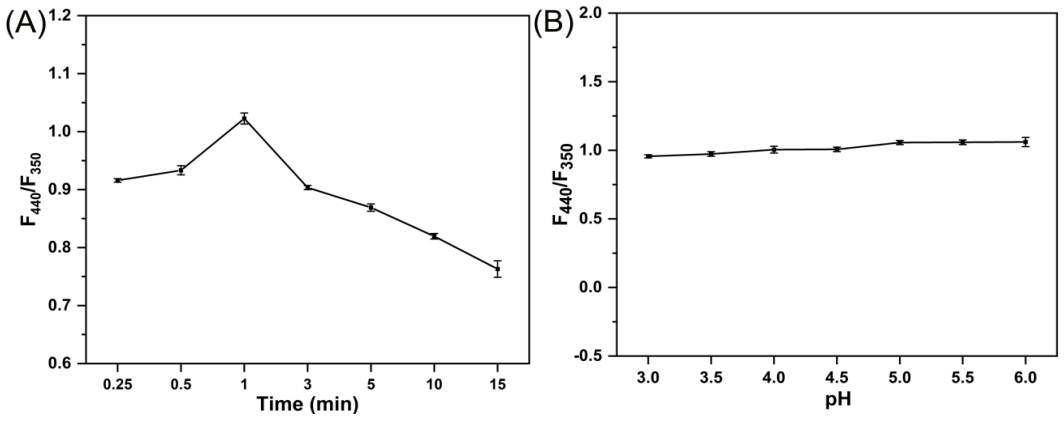

Fig. 4. Effect of (A) equilibration time and (B) pH on the response value (F_{440}/F_{350}) of ratio sensor.

3.5. Fluorescence detection of norfloxacin

For analyzing CeO_2 QDs' capacity in detecting NOR, we examined the fluorescence spectra of a ratiometric sensor versus NOR concentration (Fig. 5A). The fluorescence intensity ratio F_{440}/F_{350} increases progressively with rising concentrations of NOR. From Fig. 5B, the strong linear relation (R^2=0.9997) was established over 1 nM to 1000 nM, represented by the fitted linear equation F_{440}/F_{350} = 0.1503 + 0.00865C, where F_{440}/F_{350} denotes the ratio of fluorescence intensities between NOR and CeO_2. The limit of detection (LOD), calculated using the formula LOD = 3δ/K, is determined to be 0.65 nM. As summarized in Table 1, the LOD for our developed fluorescence probe decreases relative to that reported by many existing approaches in detecting NOR. Consequently, this innovative fluorescence method demonstrates the extensive linear range whereas the lower LOD, indicating significant potential for determining NOR levels in water samples.

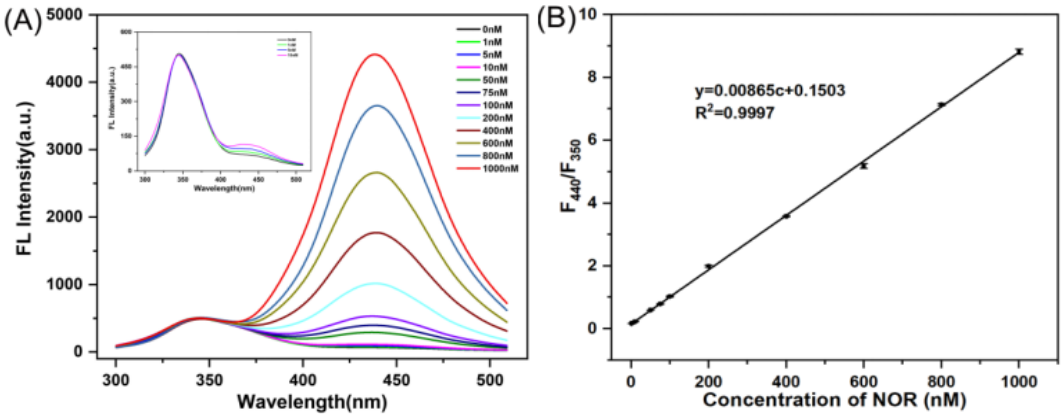

Fig. 5. (A) Fluorescence emission spectra of the ratio sensor in the presence of different concentrations of norfloxacin; (B) Plot of F_{440}/F_{350} value vs norfloxacin concentration. Experimental conditions: 1.0 μL·mL^{-1} CeO_2, 1~1000nmol/L norfloxacin, Tris-HCl buffer solution (10 mM Tris, pH =6.0) and λ_{ex}=263 nm.

To validate whether our approach was accurate, we employed high-performance liquid chromatography (HPLC). From Fig. 6A, peak height showed a gradual increase corresponding to higher concentrations of norfloxacin (NOR). Furthermore, from Fig. 6B, the wide linear association of peak area with NOR concentration was observed. The linear regression equation derived from this analysis is A = 0.3001C + 0.6394, and the correlation coefficient (R^2) was 0.9994. Both methods were compared, which indicates that they share the same linear range. Therefore, the method we have proposed is suitable for determining norfloxacin levels.

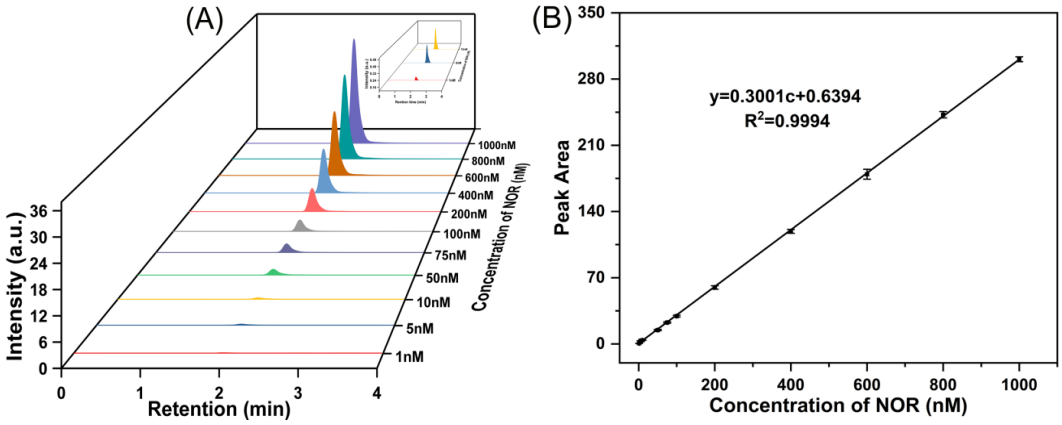

Fig. 6. Chromatogram of the different concentrations of norfloxacin; (B) Plot of peak area vs norfloxacin concentration.

Table 1. Comparison of the proposed material for NOR detection with other previously reported works.

Method	Material	Linear range (μM)	LOD (nM)	Reference
Fluorescence	Cs_2ZnCl_4	0.2 ~ 50.0	149.9	37
Electrochemical	Pd^{2+}@P-CDP/COFs	0.08~7.0 and 7.0~100.0	31	38
Electrochemical	CdTe QDs	0.2 ~ 7.4	6.6	39
Fluorescence	terbium (III)	3.13~313	0.063	40
Electrochemical	MIP/MWCNT/GCE	1.2 ~1000	40.6	41
Fluorescence	Tb/CdTe QDs	0 ~ 1.2	6.03	24
UV	FeO_x@ZnMnFeO*y*@Fe-Mn	0.41 ~ 4.71	52	42
Electrochemical	MWCNTs	0.003~0.39 and 0.39~3.13	1.58	43
Electrochemical	PAMAM-Au	3.13~31.3	1.20	44
Fluorescence	HA-GQDs-MIP	3.13 ~313	1.10	45
Fluorescence	CeO_2 QDs	0.001~1.0	0.65	This work

3.6. Selectivity of CeO_2 QDs for norfloxacin

We analyzed F_{440}/F_{350} ratios of several NOR structural analogs, like PRFX, MOX, OFL, GTFX, and SPX. From Fig. 7A, fluorescence intensity ratio is significantly elevated only in the presence of NOR, while the other analogs exhibit negligible or minimal fluorescence intensity. This indicates that NOR can be highly selectively recognized from SPX, PRFX, and other fluoroquinolones. Additionally, the influence of various cations, such as Na^+, K^+, Cu^{2+}, Fe^{3+}, Ca^{2+}, and Mg^{2+}, on CeO_2 QDs' fluorescence response was examined at a concentration of 0.10 μM. As shown in Fig. 7A, all these cations have a minor impact on the F_{440}/F_{350} value. It revealed that these potential interfering substances are mixed with CeO_2 QDs and norfloxacin, their influence on F_{440}/F_{350} value is basically consistent with that when they exist alone, as illustrated in Fig. 7B. As mentioned above, the ratiometric fluorescence sensor that we proposed has good selectivity and anti-interference ability.

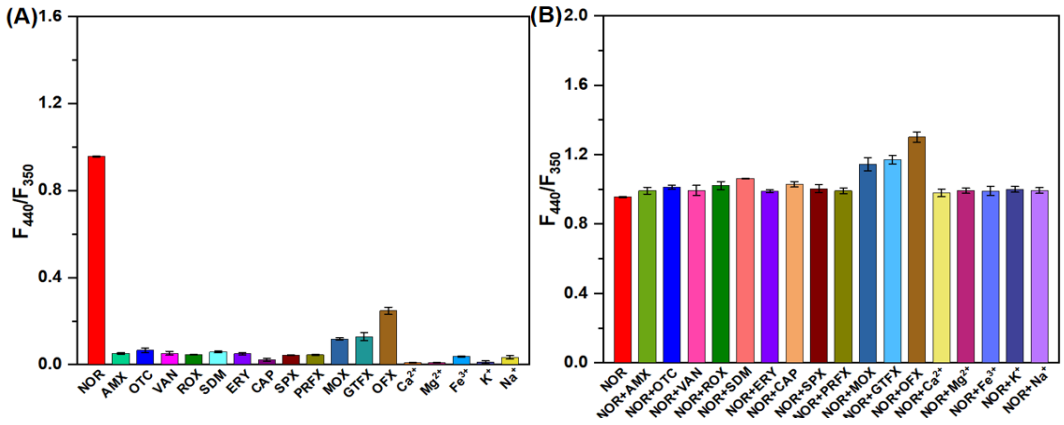

Fig. 7. Selectivity of ratio sensor for NOR over the structural analogs and the inorganic salts under the same concentrations (0.10 μM).

3.7. Norfloxacin detection in water samples

For evaluating whether this probe was practically applicable to real-world water samples, we employed CeO_2 QDs for detecting NOR within tap water, river water, lake water, and wastewater obtained in Jiaxing city. As shown in Table 2, NOR remained undetectable within any of original water samples. Subsequently, standard addition method was used to spike different concentrations (50, 200, and 600 nM) of NOR into these water samples. The NOR recovery rates were 95.54%-101.04%, and relative standard deviations (RSDs, n=3) changing between 0.46% and 3.99%. Therefore, this approach is highly recoverable, accurate and repeatable. Consequently, the CeO_2 QDs-based fluorescence probe holds significant potential for determining NOR in environmental water samples.

Table 2. Determination results for NOR residues in water samples (n = 3).

Sample	Detected (nM)	Spiked (nM)	Fluorescence			HPLC		
			Found (nM)	Recovery (%)	RSD (%)	Found (nM)	Recovery (%)	RSD (%)
Tap water	ND	50	48.91	97.83	3.45	49.07	98.15	2.38
	ND	200	192.16	96.08	2.68	198.58	99.29	2.68
	ND	600	573.22	95.54	1.64	605.78	100.96	1.86
Lake water	ND	50	50.22	100.44	2.54	48.74	97.48	1.42
	ND	200	202.08	101.04	3.48	203.13	101.57	1.18
	ND	600	600.13	100.02	3.07	614.11	102.35	2.26
Waste water	ND	50	49.16	98.32	0.46	47.96	95.93	1.45
	ND	200	196.92	98.46	1.74	200.80	100.40	2.94
	ND	600	580.61	96.77	1.38	587.23	97.87	1.09
River water	ND	50	49.50	99.01	2.56	49.07	98.15	1.41
	ND	200	201.07	100.54	2.59	203.35	101.68	1.94
	ND	600	580.28	96.71	3.99	623.33	103.89	2.09

4. Conclusion

In conclusion, we developed a facile, dual emission ultrasensitive ratio fluorescent sensor for the rapid detection of norfloxacin combined with CeO_2. Under optimized experimental conditions, norfloxacin can be detected within 60 s (pH=6.0), and the specific values of F_{440}/F_{350} exhibited excellent linear relation with norfloxacin concentration of 1.0-1000 nM, and the LOD was as low as 0.65 nM. Additionally, this ratio fluorescent sensor could be used for detecting norfloxacin within real water samples and high recoveries have been obtained in the range of 95.54%~101.04%, with relative standard deviations less than 5%. The recovery results measured by this method are basically consistent with those obtained by HPLC. Therefore, this study provides an easy and efficient method to accurately and rapidly determine norfloxacin within environmental water samples.

Acknowledgements

This work was financially supported by Jiaxing Science and Technology Project (No. 2023AY31019 and 2024AD10058).

References

[1] A. C. Fenneman, M. Weidner, L. A. Chen, M. Nieuwdorp, M. J. Blaser, Nature Reviews Gastroenterology & Hepatology, 20, 81-100 (2023); https://doi.org/10.1038/s41575-022-00685-9

[2] N. E. Frei, S. Dräger, M. Weisser, M. Osthoff, International Journal of Infectious Diseases, 124, 89-95 (2022); https://doi.org/10.1016/j.ijid.2022.09.025

[3] Y. Gorelik, S. Freilich, S. Gerassy-Vainberg, S. Pressman, C. Friss, A. Blatt, G. Focht, Y. L. Weisband, S. Greenfeld, R. Kariv, N. Lederman, I. Dotan, N. Geva-Zatorsky, S. S. Shen-Orr, Y. Kashi, Y. Chowers, Gut, 71, 287 (2022); https://doi.org/10.1136/gutjnl-2021-325185

[4] M. Gawrońska, M. Kowalik, M. Makowski, TrAC Trends in Analytical Chemistry, 155, 116691 (2022); https://doi.org/10.1016/j.trac.2022.116691

[5] L. L. Shen, W. E. Kohlbrenner, D. Weigl, J. Baranowski, Journal of Biological Chemistry, 264, 2973-2978 (1989); https://doi.org/10.1016/S0021-9258(19)81708-8

[6] Q. F. Han, X. R. Zhang, X. Y. Xu, X. L. Wang, X. Z. Yuan, Z. J. Ding, S. Zhao, S. G. Wang, Science of The Total Environment, 760, 143863 (2021); https://doi.org/10.1016/j.scitotenv.2020.143863

[7] D. G. J. Larsson, C.-F. Flach, Nature Reviews Microbiology, 20, 257-269 (2022); https://doi.org/10.1038/s41579-021-00649-x

[8] L. Dong, Y. Envelope, D. Mj, E. Ygza, D. Jw, Environment International, 158, 106949 (2022). [9] A. Gl, A. Xq, A. Jw, A. Lx, W. A. Xuan, L.A. Ying, A. Yc, B. Qla, Journal of Hazardous Materials, 436, 129107 (2022); https://doi.org/10.1016/j.jhazmat.2022.129107

[10] B. Prutthiwanasan, C. Phechkrajang, L. Suntornsuk, Talanta, 259, 74-79 (2016); https://doi.org/10.1016/j.talanta.2016.05.080

[11] L. Du, S. Ahmad, L. Liu, L. Wang, J. Tang, Science of The Total Environment, 858, 159815 (2023); https://doi.org/10.1016/j.scitotenv.2022.159815

[12] M. Amjadi, J. L. Manzoori, T. Hallaj, T. Shahbazsaghir, Microchimica Acta, 184, 1587-1593 (2017); https://doi.org/10.1007/s00604-017-2139-x

[13] X. Liu, Z. Xu, Z. Han, L. Fan, S. Liu, H. Yang, Z. Chen, T. Sun, B. Ning, Talanta, 234, 122703 (2021); https://doi.org/10.1016/j.talanta.2021.122703

[14] D. Qin, M. Zhao, J. Wang, Z. Lian, Marine Pollution Bulletin, 150, 110677 (2020); https://doi.org/10.1016/j.marpolbul.2019.110677

[15] Y. Li, J. Zhu, Y. Ma, Y. Li, J. Shao, H. Li, Journal of Environmental Chemical Engineering, 10, 108916 (2022); https://doi.org/10.1016/j.jece.2022.108916

[16] X. Qiu, J. Gu, T. Yang, C. Ma, L. Li, Y. Wu, C. Zhu, H. Gao, Z. Yang, Z. Wang, X. Li, A. Hu, J. Xu, L. Zhong, J. Shen, A. Huang, G. Chen, Spectrochimica Acta Part A: Molecular and Biomolecular Spectroscopy, 276, 121212 (2022); https://doi.org/10.1016/j.saa.2022.121212

[17] C. Liu, X. Feng, H. Qian, G. Fang, S. Wang, Food Analytical Methods, 8, 596-603 (2015); https://doi.org/10.1007/s12161-014-9936-1

[18] C. Shao, C. Li, C. Zhang, Z. Ni, X. Liu, Y. Wang, Spectrochimica Acta Part A: Molecular and Biomolecular Spectroscopy, 236, 118334 (2020); https://doi.org/10.1016/j.saa.2020.118334

[19] N. Lian, Y. Zhang, D. Liu, J. Tang, H. Wu, Microchemical Journal, 164, 105989 (2021); https://doi.org/10.1016/j.microc.2021.105989

[20] Y. Cheng, H. Wang, Y. Zhuo, D. Song, C. Li, A. Zhu, F. Long, Biosensors and Bioelectronics, 199, 113863 (2022); https://doi.org/10.1016/j.bios.2021.113863

[21] H. Lu, S. Quan, S. Xu, Journal of Agricultural and Food Chemistry, 65, 9807-9814 (2017); https://doi.org/10.1021/acs.jafc.7b03986

[22] S. Wang, X. Bao, B. Gao, M. Li, Dalton Transactions, 48, 8288-8296 (2019); https://doi.org/10.1039/C9DT01186B

[23] T. Shi, H. Fu, L. Tan, J. Wang, Microchimica Acta, 186, 362 (2019); https://doi.org/10.1007/s00604-019-3440-7

[24] R. Jiang, D. Lin, Q. Zhang, L. Li, L. Yang, Sensors and Actuators B: Chemical, 350, 130902 (2022); https://doi.org/10.1016/j.snb.2021.130902

[25] C. Ye, X. Chen, D. Zhang, J. Xu, H. Xi, T. Wu, D. Deng, C. Xiong, J. Zhang, G. Huang, Electrochimica Acta, 379, 138174 (2021); https://doi.org/10.1016/j.electacta.2021.138174

[26] Y. Xu, Y. Lin, N. Chu, Y. Xing, X. Chen, Chemical Engineering Journal, 435, 134907 (2022); https://doi.org/10.1016/j.cej.2022.134907

[27] S. Hu, J. Liu, G. Zhang, Z. Wang, X. Xiao, D. Li, J. Peng, W. Lai, Talanta, 219, 121245 (2020); https://doi.org/10.1016/j.talanta.2020.121245

[28] M. Yang, H. Li, J. Liu, W. Kong, S. Zhao, C. Li, H. Huang, Y. Liu, Z. Kang, Journal of Materials Chemistry B, 2, 7964-7970 (2014); https://doi.org/10.1039/C4TB01385A

[29] F. Maleki, A. Daneshfar, New Journal of Chemistry, 46, 22692-22702 (2022); https://doi.org/10.1039/D2NJ04429C

[30] X. Wei, Z. Zhou, T. Hao, H. Li, J. Dai, L. Gao, X. Zheng, J. Wang, Y. Yan, Journal of Luminescence, 161, 47-53 (2015); https://doi.org/10.1016/j.jlumin.2014.12.050

[31] L. Li, Y. Cheng, Y. Ding, S. Gu, F. Zhang, W. Yu, European Journal of Inorganic Chemistry, 2013, 2564-2570 (2013); https://doi.org/10.1002/ejic.201201372

[32] B. B. Chen, M. L. Liu, C. M. Li, C. Z. Huang, Advances in Colloid and Interface Science, 270, 165-190 (2019); https://doi.org/10.1016/j.cis.2019.06.008

[33] B. Wkla, B. Jtfa, B. Zqma, Carbon, 161, 685-693 (2020); https://doi.org/10.1016/j.carbon.2020.01.098

[34] P. Modlitbová, P. Pořízka, K. Novotný, J. Drbohlavová, I. Chamradová, Z. Farka, H. Zlámalova-Gargošová, T. Romih; J. Kaiser, Ecotoxicology and Environmental Safety, 153, 23-31 (2018); https://doi.org/10.1016/j.ecoenv.2018.01.044

[35] J. Tian, W. Wei, J. Wang, S. Ji, G. Chen, J. Lu, Analytica Chimica Acta, 1000, 265-272 (2017); https://doi.org/10.1016/j.aca.2017.08.018

[36] H. Xu, H. Wang, Y. Lu, Y. Zeng, Y. Yang, Z. Zhang, H. Wang, X. Wang, L. Li, Spectrochimica acta. Part A, Molecular and biomolecular spectroscopy, 262, 120115 (2021); https://doi.org/10.1016/j.saa.2021.120115

[37] N. Yang, Q.-L.Wen, Y.-B. Fu, L.-F. Long, Y.-J. Liao, S.-B. Hou, P. Qian, P. Liu, J. Ling, Q. Cao, Spectrochimica Acta Part A: Molecular and Biomolecular Spectroscopy, 281, 121568 (2022); https://doi.org/10.1016/j.saa.2022.121568

[38] C. Zhang, L. Fan, J. Ren, M. Cui, N. Li, H. Zhao, Y. Qu, X. Ji, Journal of Pharmaceutical and Biomedical Analysis, 219, 114956 (2022); https://doi.org/10.1016/j.jpba.2022.114956

[39] A. M. Santos, A. Wong, F. H. Cincotto, F. C. Moraes, O. Fatibello-Filho, Microchimica Acta, 186, 148 (2019); https://doi.org/10.1007/s00604-019-3268-1

[40] J. Chen, Y. Jin, T. Ren, S. Wang, X. Wang, F. Zhang, Y. Tang, Food Chemistry, 386, 132751 (2022); https://doi.org/10.1016/j.foodchem.2022.132751

[41] H. da Silva, J. Pacheco, J. Silva, S. Viswanathan, C. Delerue-Matos, Sensors and Actuators B: Chemical, 219, 301-307 (2015); https://doi.org/10.1016/j.snb.2015.04.125

[42] M. Sun, M. He, S. Jiang, Y. Wang, X. Wang, T. Liu, C. Song, S. Wang, H. Rao, Z. Lu, Chemical Engineering Journal, 425, 131823 (2021); https://doi.org/10.1016/j.cej.2021.131823

[43] Z. Liu, M. Jin, H. Lu, J. Yao, X. Wang, G. Zhou, L. Shui, Sensors and Actuators B: Chemical, 288, 363-372 (2019); https://doi.org/10.1016/j.snb.2019.02.097

[44] B. Liu, M. Li, Y. Zhao, M. Pan, Y. Gu, W. Sheng, G. Fang, S. Wang, Sensors, 18, 1946 (2018); https://doi.org/10.3390/s18061946

[45] O. Bunkoed, P. Donkhampa, P. Nurerk, Microchemical Journal, 158, 105127 (2020); https://doi.org/10.1016/j.microc.2020.105127